



**HAL**  
open science

# Coccolith $\delta^{18}\text{O}$ and alkenone records in middle Pliocene orbitally controlled deposits: High-frequency temperature and salinity variations of sea surface water

Catherine Beltran, Marc de Rafélis, Fabrice Minoletti, Maurice Renard,  
Marie-Alexandrine L Sicre, Ullah Ezat

## ► To cite this version:

Catherine Beltran, Marc de Rafélis, Fabrice Minoletti, Maurice Renard, Marie-Alexandrine L Sicre, et al.. Coccolith  $\delta^{18}\text{O}$  and alkenone records in middle Pliocene orbitally controlled deposits: High-frequency temperature and salinity variations of sea surface water. *Geochemistry, Geophysics, Geosystems*, 2007, 8 (5), 10.1029/2006gc001483 . hal-03190122

**HAL Id: hal-03190122**

**<https://hal.science/hal-03190122>**

Submitted on 6 Apr 2021

**HAL** is a multi-disciplinary open access archive for the deposit and dissemination of scientific research documents, whether they are published or not. The documents may come from teaching and research institutions in France or abroad, or from public or private research centers.

L'archive ouverte pluridisciplinaire **HAL**, est destinée au dépôt et à la diffusion de documents scientifiques de niveau recherche, publiés ou non, émanant des établissements d'enseignement et de recherche français ou étrangers, des laboratoires publics ou privés.



## Coccolith $\delta^{18}\text{O}$ and alkenone records in middle Pliocene orbitally controlled deposits: High-frequency temperature and salinity variations of sea surface water

Catherine Beltran, Marc de Raféllis, Fabrice Minoletti, and Maurice Renard

*Laboratoire Biominéralisations et Paléoenvironnements, JE 2477, Université Pierre et Marie Curie, Case 116, 4 Place Jussieu, F-75252 Paris Cedex 05, France (beltran@ccr.jussieu.fr)*

Marie Alexandrine Sicre and Ullah Ezat

*Laboratoire des Sciences du Climat et de l'Environnement, Domaine du CNRS, Avenue de la Terrasse, F-91198 Gif-sur-Yvette Cedex, France*

[1] The calcareous nanoplankton flora is strongly controlled by water masses and is sensitive to ambient nutrient levels. In consequence, fossil remains of calcareous nanoplankton are useful tools for paleoceanography. Although they are the major producers of carbonates in the pelagic realm, their use as a seawater  $\delta^{18}\text{O}$  recorder is not easy due to their small size and the difficulty in isolating them from the bulk carbonate. Using a granulometric separation technique (Minoletti et al., 2001), it is now possible to concentrate coccoliths in monospecific fractions. We applied this method on three precession cycles (insolation cycles i-288 to i-282) from the mid-Pliocene Punta Piccola section (South Sicily), which led to an almost pure *Pseudoemiliana lacunosa* fraction. It was then possible to measure the isotopic signatures ( $\delta^{18}\text{O}$  and  $\delta^{13}\text{C}$ ) and alkenone unsaturation ratio on the same recorder: *P. lacunosa*. This permits a precise reconstruction of environmental conditions (temperature and salinity) that prevailed in the upper photic zone during the cyclic deposition of these sediments. Our data provide a clear confirmation that sapropelic marl formation occurred during a wetter climate compared to the deposition of the marly limestones. Moreover, these results point out that salinity variations are not, as previously thought, always the primary factor that controlled the deposition of these cyclic events. This study is a step forward in the utilization of calcareous nanoplankton isotopic records in paleoenvironmental reconstructions.

**Components:** 7929 words, 7 figures, 3 tables.

**Keywords:** Pliocene; sapropels; Mediterranean; stable isotopes; alkenone; calcareous nanofossils.

**Index Terms:** 0473 Biogeosciences: Paleoclimatology and paleoceanography (3344, 4900).

**Received** 13 September 2006; **Revised** 18 January 2007; **Accepted** 31 January 2007; **Published** 5 May 2007.

Beltran, C., M. de Raféllis, F. Minoletti, M. Renard, M. A. Sicre, and U. Ezat (2007), Coccolith  $\delta^{18}\text{O}$  and alkenone records in middle Pliocene orbitally controlled deposits: High-frequency temperature and salinity variations of sea surface water, *Geochem. Geophys. Geosyst.*, 8, Q05003, doi:10.1029/2006GC001483.

## 1. Introduction

[2] Pliocene Mediterranean deposits usually display rhythmic bedding of carbonate-rich and carbonate-poor alternations. Some dark or black layers are even so rich in organic matter that they sometimes reach true sapropel concentration levels [Kidd *et al.*, 1978]. However, in continental outcrops, such high-organic matter concentrations are rarely reached due to oxidation after exposure and the term “sapropelic marl” appears more appropriate. Kullenberg [1952] was the first to attribute this concentration of organic matter to increased rainfall and runoff into the Mediterranean Sea. The effects of increased freshwater supply to the Mediterranean Sea may have been (1) the development of a low-salinity surface layer, resulting in reduced deep-water circulation, and (2) the delivery of an increased amount of nutrients from the continents, thus enhancing productivity [Rohling and Gieskes, 1989; Rohling and Hilgen, 1991; Rohling, 1994]. These phenomena lead to hydrological stratification, causing anoxia of bottom waters, which engenders the preservation of organic matter before its burial. The rhythmic sequences, which include sapropelic beds, were already explained by a climatic control of orbitally forced insolation variations [Rossignol-Strick, 1983, 1985; Hilgen, 1991]. However, the importance of salinity versus temperature effect on the formation of these organic-rich layers still has to be refined. The aim of this study is to evaluate the respective role of these two parameters during the deposition of three Pliocene sedimentary cycles from the Punta Piccola section (southern Sicily).

[3] Classically, paleoenvironmental reconstructions are performed using  $\delta^{18}\text{O}$  values of planktonic foraminifera and the  $U_{37}^k$  index which is a proxy of sea-surface temperatures (SST). However, these methods mix data related to different water mass characteristics, since the calcification season and the depth habitat of planktonic foraminifera ( $\delta^{18}\text{O}$ ) can differ from the growth season and the depth of calcification of the phytoplankton producing alkenones.

[4] Although calcareous nannofossils are the major producers of carbonates and alkenones in the pelagic realm, the use of coccoliths as seawater  $\delta^{18}\text{O}$  recorder is not easy due to their small size and the difficulty in isolating them from the bulk carbonate. In this study, a new granulometric separation technique [Minoletti *et al.*, 2001, 2005] is used to concentrate coccoliths, which

allows the measurement of their  $\delta^{18}\text{O}$  based on monospecific coccolith fraction. The alkenone unsaturation ratios are used to determine the SST and the combination of the alkenone-derived SST and the  $\delta^{18}\text{O}$  values of coccoliths are used to resolve sea-surface paleosalinity.

## 2. Geological Setting

[5] The Capo Rossello composite section [Cita and Gartner, 1973] is considered as the reference for the Mediterranean lower-middle Pliocene chronostratigraphy [Langereis and Hilgen, 1991]. In particular, the Monte Narbone Formation sedimentary cycles from the Punta Piccola section [Brolsma, 1978; Hilgen, 1987] are strongly related to precession astronomical variations [Rossignol-Strick, 1985; Hilgen, 1991] and enabled the establishment of a cyclochronology of the middle Pliocene [Langereis and Hilgen, 1991; Lourens *et al.*, 1996]. The Punta Piccola section outcrops along the southern Sicilian coast, near Porto Empedocle. Our study (Figure 1) is focused on cycles 104 to 107 of Langereis and Hilgen [1991] spanning the period between 3.01 and 2.95 Myr [Lourens *et al.*, 1996]. It consists of meter-thick, gray marly limestones ( $50\% \leq \text{CaCO}_3 \leq 60\%$ ), alternating regularly with 0.5 m thick brown sapropelic marls ( $42\% \leq \text{CaCO}_3 \leq 51\%$  and  $\text{TOC} \sim 0.5\%$ ). The sapropelic semi-couplet of cycle 107 corresponds to the “layer-G” described by Brolsma [1978].

[6] Many paleoenvironmental, chemical and mineralogical studies have previously been performed on these orbitally driven deposits consisting of alternating sapropelic marls and marly limestones. According to Foucault and Mélières [2000], the non-calclitic phase of the sediments is mainly composed of quartz, dolomite and clays with relative proportions that vary cyclically. The marly limestones are characterized by the clay mineral assemblages of palygorskite, kaolinite and illite, while the sapropelic marls yield higher proportions of smectite and chlorite. The authors have attributed these cyclic variations to climatic alternation of weak and strong rainfall periods, which may have controlled sea surface salinity variations.

[7] The calcitic fraction consists essentially of calcareous nannofossils and planktonic foraminifera. The recent work of Sprovieri *et al.* [2006], using a high-resolution quantitative analysis of the planktonic assemblages from the Punta Piccola section, shows that the foraminifera distributions record astronomical periodicities. They note that

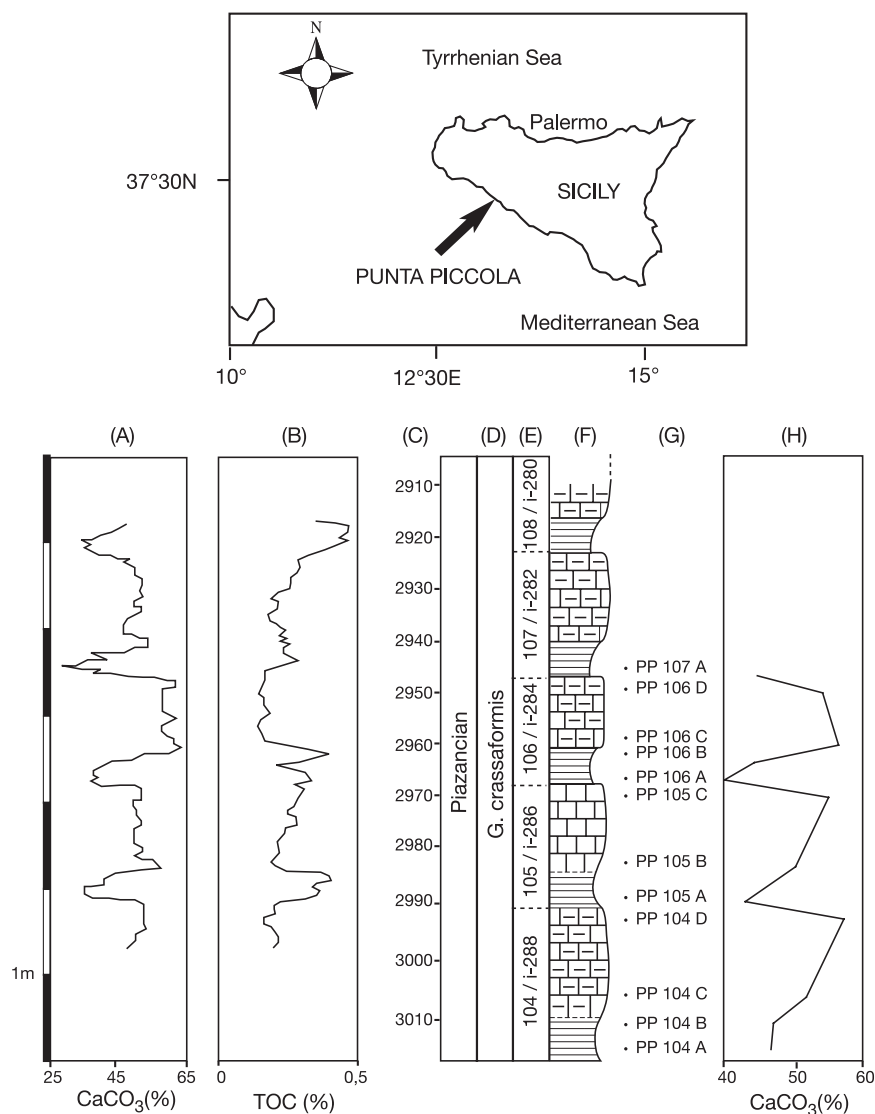


**Figure 1.** Localization and schematic representation of the Punta Piccola section. Figures 1a and 1b correspond to the CaCO<sub>3</sub> and TOC fluctuations in the cycles studied by *Foucault and Mélières* [2000]. Figure 1c is the *Lourens et al.* [1996] astronomical timescale (ka). Figure 1d is the foraminifera zone [*Spaak*, 1983]. The references to *Langereis and Hilgen* [1991] astronomical cycles 104 to 107 and to *Lourens et al.* [1996] insolation cycles (i-288 to i-280) are reported in Figure 1e. Figure 1f represents the lithological profile of the Punta Piccola section. In Figures 1g and 1h are reported the sample names and positions and the CaCO<sub>3</sub> variations throughout the section selected for this study.

*Globigerinoides obliquus* and *Globigerinoides quadrilobus* appear to be primarily controlled by precession, whereas *Globigerinoides ruber* is largely forced by obliquity.

### 3. Methods

#### 3.1. Separation of the Homogeneous Fine Fractions

[8] The protocol for the separation of homogeneous fine fractions used to concentrate the cocco-

lith fraction is described by *Minoletti et al.* [2001, 2005]. This method, based on granulometric separations of the various carbonate particles, was applied to samples from both lithologies described above. The protocol can be split into three parts (see Figure S1)<sup>1</sup>. The preliminary phase is a soft disaggregation of the rock followed by wet sieving in order to remove the microfossils of >200  $\mu\text{m}$ , consisting mainly of planktic foraminifera

<sup>1</sup>Auxiliary material data sets are available at <ftp://ftp.agu.org/apend/gc/2006gc001483>. Other auxiliary material files are in the HTML.

**Table 1.** Mean Composition of Separated Fractions of Each Lithology<sup>a</sup>

Granulometric Fractions	Foraminifera		Coccoliths		<i>Reticulofenestra</i> spp.		<i>P. lacunosa</i>		<i>Discosaster</i> spp.		Micarb	
	ML	SM	ML	SM	ML	SM	ML	SM	ML	SM	ML	SM
(>12 $\mu\text{m}$ )	70%	90%	20%	4%							10%	6%
(12–5 $\mu\text{m}$ )	25%	38%	40%	28%							30%	28%
(5–3 $\mu\text{m}$ )	15%	15%	21%	21%					5%	6%	54%	57%
(<3 $\mu\text{m}$ )			4%	7%	16%	13%	80%	80%	10%	7%		

<sup>a</sup> ML, Marly limestone; SM, sapropelic marls.

(e.g., *Orbulina universa*). Subsequently, the resulting suspension is finely separated by successive filtration steps with membranes of decreasing opening size (12, 5 and 3  $\mu\text{m}$ ). After separation, the residues were dried and weighed in order to evaluate their respective mass percentage of the bulk sediment (see Figure S1).

[9] Smear slides are prepared from each separated fraction. In each fraction, the surface area of 200 randomly selected carbonate particles is measured in light microscopy using a cross-grid graticule to quantify the composition of each fraction. The particle volume is evaluated by combining the particle surface area and its mean thickness determined by scanning electron microscopy observations. Assuming that the density of all carbonate minerals is homogeneous, this method leads to a relative weight estimation of the different carbonate particle types in each fraction. On the basis of replicate counts, the cumulative error for any given component is less than 10% [Minoletti, 2002].

[10] This method, which has already been successfully applied in other studies [Minoletti *et al.*, 2005; Stoll and Bains, 2003], allows one to obtain two kinds of fine fractions: (1) the so-called pure fractions, in which one carbonate particle type represents up to 80% of the carbonate fraction, and (2) the mixed fractions, in which two or three major carbonate components coexist.

### 3.2. Stable Isotope Measurements

[11] The oxygen and carbon isotopic composition of bulk carbonates and the separated fractions were measured on all samples. The extraction of  $\text{CO}_2$  was done by reaction with anhydrous orthophosphoric acid at 50°C. The analysis was performed with a mass spectrometer Finnigan Delta E. The oxygen and carbon isotope values are expressed in per mil relative to the V-PDB standard reference. The analytical precision is estimated at 0.1‰ for oxygen and 0.05‰ for carbon.

### 3.3. Alkenone Analyses

[12] The alkenone insaturation index was determined for 12 samples (6 from sapropelic marls and 6 from marly limestones), chosen according to their bulk oxygen isotope values. Lipid extracts were partitioned into compound classes following the procedure of *Ternois et al.* [1997]. Alkenones were isolated on silica gel, using solvents of increasing polarity. The fractions containing the alkenones were concentrated, transferred to vials

**Table 2.** Mean Composition of Carbonate Phase Related to Lithology<sup>a</sup>

Lithology	Foraminifera		Coccoliths		<i>Discoaster</i> spp.	Micarb
Marly limestone	<b>16%</b> (12–20%)		<b>70%</b> (65–80%)		<b>2%</b> (1.5–5%)	<b>12%</b> (6–15%)
		<i>P. lacunosa</i>	<i>Reticulofenestra</i> spp.	Other		
		48% (40–60%)	8% (5–10%)	14% (5–20%)		
Sapropelic marl	<b>20%</b> (18–23%)		<b>65%</b> (59–75%)		<b>3%</b> (0–6%)	<b>12%</b> (6–18%)
		<i>P. lacunosa</i>	<i>Reticulofenestra</i> spp.	Other		
		45% (35–55%)	10% (5–16%)	10% (3–15%)		

<sup>a</sup>The mean values are in bold, and the range of values is in parentheses.

and evaporated under a nitrogen stream. They were then dissolved in hexane and analyzed on a Varian 3400 series equipped with a fused silica capillary column (CP Sil 8, 50 length, 0.32 mm internal diameter, 0.25  $\mu\text{m}$  film thickness) and a flame ionization detector. Helium was used as a carrier gas. Peak areas were used to calculate the  $U_{37}^k$  index:  $U_{37}^k = C_{37:2}/(C_{37:2} + C_{37:3})$ , according to Brassell *et al.* [1986]. The  $5\alpha$ -cholestane was used as an external standard.

## 4. Results

### 4.1. Paleontological Composition of Carbonate Fraction of the Various Lithologies

[13] Three filtration steps were performed to separate the following four fractions (Table 1, Table S1, and Figure S1): (1) the  $>12 \mu\text{m}$  fraction which concentrates foraminifera debris; (2) the  $12\text{--}5 \mu\text{m}$  fraction, mainly composed of polyspecific coccolith assemblages (mainly *Pontosphaera* spp., *Calcidiscus* spp., *Helicosphaera* spp., *Coccolithus pelagicus*, *Scyphosphaera* spp., *Discoaster* spp.), foraminifera debris and “micarb particles” (in the sense of Noël *et al.* [1994] and Mattioli and Pittet [2002]); (3) the  $5\text{--}3 \mu\text{m}$  fraction which contains “micarb particles” and the same polyspecific coccolith assemblage in different relative abundance, and (4) the  $<3 \mu\text{m}$  fraction is composed of up to 90% of placolith-bearing species belonging to the Noelaerhabdaceae family: *Pseudoemiliana lacunosa* and small *Reticulofenestra* spp. ( $<3 \mu\text{m}$ ), the remainder consisting of coccolith debris.

[14] Although the mean dimension of *Pseudoemiliana lacunosa* is about  $5 \mu\text{m}$  [Bown, 1998], this

species is concentrated in the ( $<3 \mu\text{m}$ ) fraction. It must be noted that during the separation protocol, particles are discriminated according to their two smaller dimensions, i.e., width and thickness (maximum  $3 \mu\text{m}$  and  $1.5 \mu\text{m}$ , respectively, for *Pseudoemiliana lacunosa*; see Figure S1). This explains why  $5 \mu\text{m}$ -long coccoliths can be collected in the fine fraction.

[15] The quantitative estimates of the carbonate fractions compositions, presented in Table 2, show that both the marly limestones and the sapropelic marls consist essentially of calcareous nannofossils (mainly *Pseudoemiliana lacunosa*), planktonic foraminifera and to less extent, of micarb.

### 4.2. Stable Isotopes

[16] For all the studied samples, the oxygen isotopic signatures of bulk carbonate, the planktic foraminifera *Orbulina universa* and the biogenic-dominated fractions ( $12\text{--}5 \mu\text{m}$  and  $<3 \mu\text{m}$ ) display similar trends throughout the section (Figures 2a and 2d; Table S1). The fine fraction ( $<3 \mu\text{m}$ ) is dominated by Noelaerhabdaceae species (on average, 80% of *Pseudoemiliana lacunosa* and 10% of small *Reticulofenestra* spp.). Moreover, both species display the same ecological preferences [Okada and Honjo, 1973]; we then make the assumption that the isotopic signature of the fine fraction is representative of that of *Pseudoemiliana lacunosa*.

[17] The marly limestone bulk carbonates have a mean  $\delta^{18}\text{O}$  value of about ‰ (range: 0.7‰–1.2‰), while the sapropelic marls have a mean  $\delta^{18}\text{O}$  value of approximately 0.3‰ (range: 0.01‰–0.5‰). The fine fraction ( $<3 \mu\text{m}$ ) exhibits higher  $\delta^{18}\text{O}$  than bulk carbonates, around 1.9‰

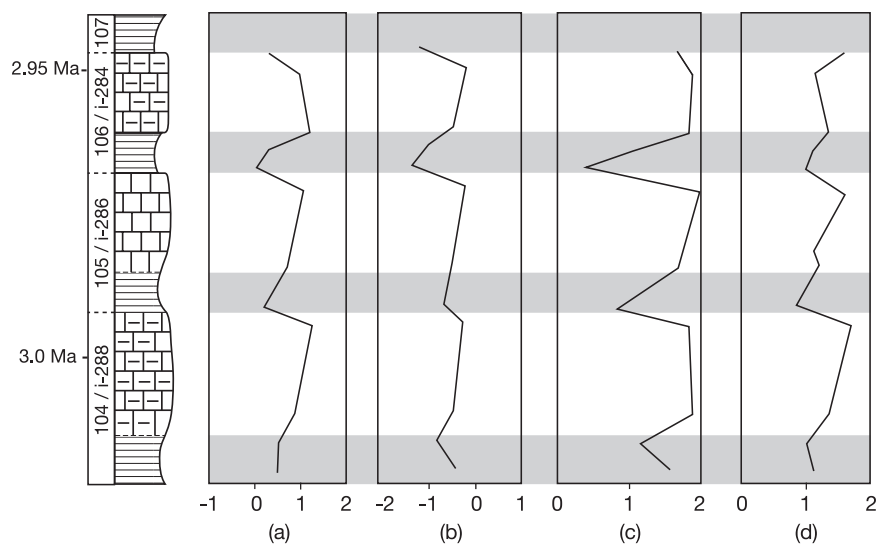


**Figure 2.** Oxygen isotopic ratios (‰ PDB) of (a) bulk carbonate, (b) (12–5  $\mu\text{m}$ ) fraction, (c) *Pseudoemiliana lacunosa* (<3  $\mu\text{m}$  fraction), and (d) *Orbulina universa*.  $\delta^{18}\text{O}$  of bulk carbonate and biogenic fractions display parallel trends according to lithology, with the highest values recorded in the marly limestones semi-couplets. The Lourens *et al.* [1996] astronomical timescale (ka) and insolation cycles (i-288 to i-280) and the Langereis and Hilgen [1991] astronomical cycles 104 to 107 are reported.

(range: 1.7‰–2.0‰) in the marly limestones and of  $\sim 1\%$  (range: 0.4‰–1.6‰) in the sapropelic marls. *Orbulina universa* have a mean  $\delta^{18}\text{O}$  value of 1.3‰ (range: 1.1‰–1.5‰) in the marly limestones, compared to 1.1‰ (range: 0.8‰–1.4‰) in the sapropelic marls layers.

[18] Negative carbon isotope shifts are recorded by bulk carbonate (mean value for sapropelic marls:  $-0.32\%$ , and marly limestones:  $0.13\%$ ) as well as for the biogenic dominated fractions in all the sapropelic layers studied (see Table S1 and Figure 3).

[19] For the fine fraction, the mean value in the marly limestones is  $0.94\%$  (range:  $0.9\%$ – $1\%$ ), whereas in the sapropelic marls, the mean value is  $0.55\%$  (range:  $0.3\%$ – $0.8\%$ ). The  $\delta^{13}\text{C}$  of *Orbulina universa* recorded is  $\sim 1.88\%$  (range:  $1.7\%$ – $1.9\%$ ) in the marly limestones and  $1.37\%$  (range:  $1.2\%$ – $1.7\%$ ) in the sapropelic marls. This feature, already noted by many authors [e.g., Bernasconi and Pika-Biolzi, 2000], has been explained by a fertility increase through the input of nutrients into the photic zone.

### 4.3. Alkenones

[20] Alkenone concentrations ( $\text{C}_{37:3}$  and  $\text{C}_{37:2}$ ) vary between 12.1 and 190.1 ng/g of dry weight sediment. The range of  $\text{U}^{k'}_{37}$  values vary between

0.82 and 0.96 (Table S1). The sapropelic marls have higher values (0.92 to 0.96) in comparison with the marly limestones (from 0.82 and 0.90).

## 5. Discussion

### 5.1. Stable Isotope Results

[21] The positive correlation between the  $\delta^{18}\text{O}$  and  $\delta^{13}\text{C}$  values is a prominent feature of our record (Figure 4). Short-term fluctuations toward lighter  $\delta^{18}\text{O}$  and  $\delta^{13}\text{C}$  values during the Pliocene are usually related to sapropelitic sediments and considered to be caused by salinity stratification during periods of increased continental run-off [Van der Zwaan and Gudjonsson, 1986].

[22] The oxygen and carbon isotope ratios recorded in the samples from the Punta Piccola section are in agreement with the values already published by Howell *et al.* [1998], for the same period for the planktic foraminifera *Globigerina bulloides* in the ODP site 964 (Ionian Sea). Because the deep sea sequences are considered to have undergone minimal post-depositional alteration by diagenesis and weathering [Thierstein and Roth, 1991], we assume that diagenetic processes have no significant overprint on the isotopic data measured in our study. Moreover, no evidence for overgrowth or dissolution were detected in microscopic observa-

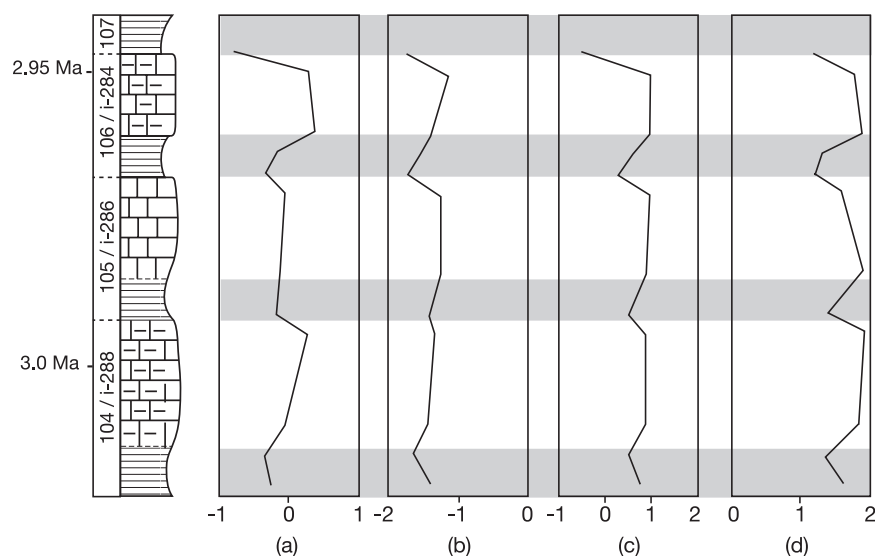


**Figure 3.** Carbon isotopic ratios (‰ PDB) of (a) bulk carbonate, (b) (12–5  $\mu\text{m}$ ) fraction, (c) *Pseudoemiliana lacunosa* (<3  $\mu\text{m}$  fraction), and (d) *Orbulina universa*. The Lourens *et al.* [1996] astronomical timescale (ka) and insolation cycles (i-288 to i-280) and the Langereis and Hilgen [1991] astronomical cycles 104 to 107 are reported.

tions. Therefore it can be assumed that the observed oxygen isotope trends registered by the Noelaerhabdaceae-dominated fine fraction and *Orbulina universa* are linked to changes in environmental parameters.

## 5.2. Bathymetric Distribution of Foraminifera and Coccoliths in the Middle Pliocene Mediterranean Sea Deducted From Oxygen Isotopic Data

[23] The mean  $\delta^{18}\text{O}$  values of the planktic foraminifera *Orbulina universa* (1.17‰) and the *Pseudoemiliana lacunosa* dominated-fraction (1.5‰), are significantly higher than the  $\delta^{18}\text{O}$  values published for *Globigerinoides obliquus* (on average  $-0.14\text{‰}$  in marly limestones and  $-1.63\text{‰}$  in sapropelic marls [Gudjonsson and Van der Zwaan, 1985]) from the Punta Piccola section.

[24] One explanation for these isotopic differences registered between *P.lacunosa*, *G.obliquus* and *O.universa* is the non-equilibrium isotopic fractionation induced by physiological factors. This species-specific isotopic disequilibrium was already recognized for several species of planktic foraminifera [see Spero and Lea, 1996; Bemis *et al.*, 2000] and calcareous nannoplankton [Dudley *et al.*, 1980, 1986]. For example, modern cultured species of coccolithophores fall into two distinct groups of temperature-dependence  $\delta^{18}\text{O}$  disequi-

librium: isotopically “heavy” and “light” groups [Dudley *et al.*, 1980, 1986]. The “heavy”  $\delta^{18}\text{O}$  group in the Dudley *et al.* [1986] experiments relates to *Emiliana huxleyi* and *Gephyrocapsa oceanica* which are the most abundant coccolithophore species in the modern ocean. Today, the production and export flux of the “light”  $\delta^{18}\text{O}$  coccolith species, such as *Cricosphaera carterae*,

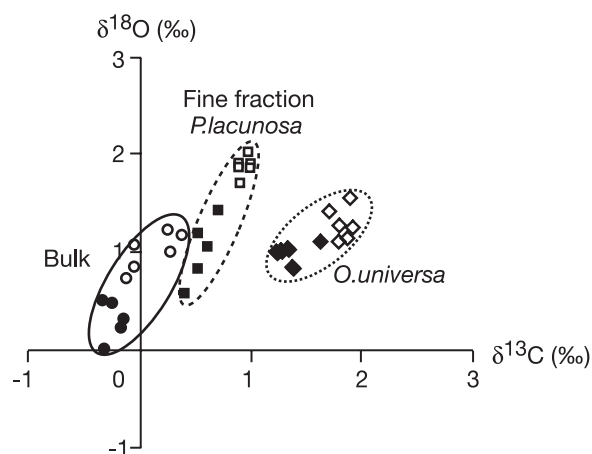


**Figure 4.** Oxygen and carbon isotopic compositions of bulk carbonate and biogenic dominated fractions. Black full and open symbols represent the isotopic values in sapropelic marls and marly limestones, respectively.



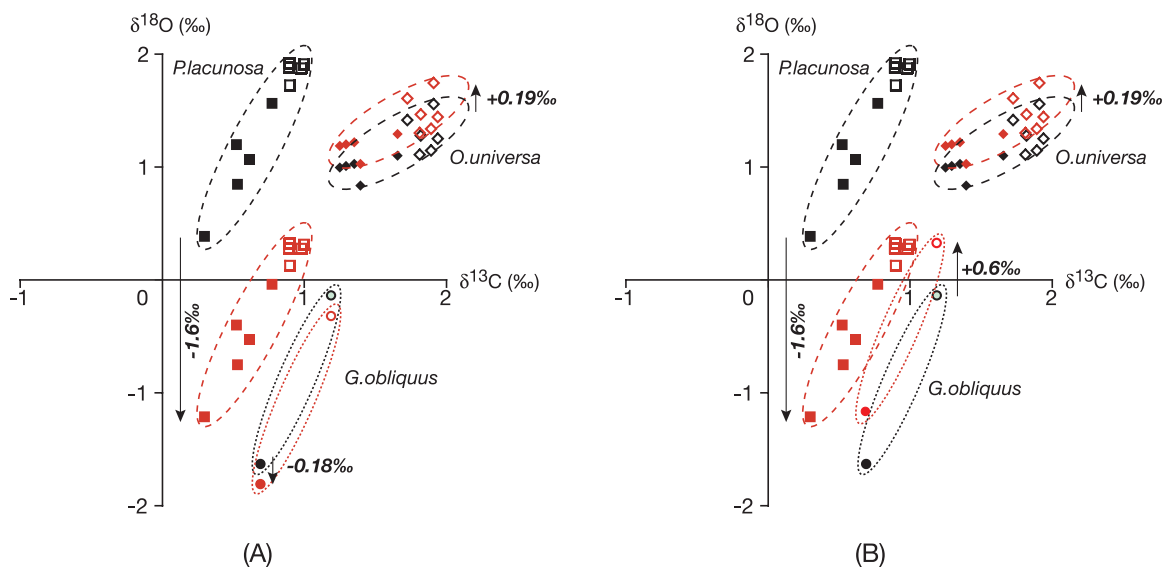


**Figure 5.** Oxygen and carbon isotopic compositions of biogenic carbonates. Black full and open symbols represent the isotopic values of sapropelic marls and marly limestones, respectively. Red full and open symbols represent the isotopic values in sapropelic marls and marly limestones, respectively, corrected from vital effects (arrows). (a) *Globigerinoides obliquus* vital-effect correction following Erez and Luz [1983]. (b) *Globigerinoides obliquus* vital-effect correction following Rohling et al. [2004].

*Calcidiscus leptoporus*, *Umbellosphaera hulburtiana* and *Umbellosphaera sibogae* [Dudley et al., 1986] are much smaller than for the heavy group in subtropical waters [Reid, 1980; Broerse et al., 2000; Haidar and Thierstein, 2001]. Although the nannoplankton species cultured by Dudley et al. [1980] and Dudley et al. [1986] are modern species, similar oxygen isotopic disequilibria might have existed in the dominant nannoplankton species during Pliocene. Since *Pseudoemiliana lacunosa* and *Reticulofenestra* spp. belong to the same family as *Emiliana huxleyi* and *Gephyrocapsa oceanica* and are the dominant coccolithophore species in the samples, we will assume that their vital effect is similar to that of *Emiliana huxleyi* (+1.6‰ [Dudley and Nelson, 1989]).

[25] The planktic foraminifera *Globigerinoides* spp. and *Orbulina universa* are considered by Erez and Luz [1983] and Ortiz et al. [1996] to produce calcite in near equilibrium with oxygen isotopic compositions of the ambient water (+0.18‰ for *Globigerinoides* spp. and -0.19‰ for *Orbulina universa*).

[26] Assuming that these corrections for the disequilibrium vital-effect with respect to the  $\delta^{18}\text{O}$  are appropriate for the Pliocene species investigated,

there is still a difference remaining between *Globigerinoides obliquus*, *Pseudoemiliana lacunosa* and *Orbulina universa* isotopic signatures (Figure 5a). The corrected *Pseudoemiliana lacunosa*  $\delta^{18}\text{O}$  values lie between those of *Globigerinoides obliquus* and *Orbulina universa* (Figure 5a).

[27] These discrepancies in isotopic data between nanofossils and planktic foraminifera can be linked to the properties of the waters in which plankton skeletal carbonate precipitated, i.e., the difference in depth habitat and growth season. Investigations from plankton tow data have shown that planktic foraminifera live vertically dispersed in the upper water column and that the depth range has a significant influence on the oxygen isotope composition of individual species [Fairbanks and Wiebe, 1980]. The living species *Orbulina universa* is known to be an intermediate dwelling species [Bernasconi and Pika-Biolzi, 2000], whereas the living planktic foraminifer *Globigerinoides* spp. [Erez and Honjo, 1981; Ravelo and Fairbanks, 1992] and its fossil analogs [Pearson and Shackleton, 1995] are regarded as being shallow mixed-layer dwellers. When considering that the  $\delta^{18}\text{O}$  primarily reflects depth calcification, our results then suggest that *Globigerinoides obliquus* calcified closer to the

sea surface than *Orbulina universa*, which is in good agreement with the later published ecological data.

[28] Coccolithophores dwell and secrete coccolith plates only within the photic zone [Okada and Honjo, 1973] and thus carry an isotopic signal characteristic of the shallow mixed layer [Goodney et al., 1980; Dudley et al., 1980, 1986].

[29] This implies that the depth habitat for the nanoplankters is very close to that of the surface-dwelling planktic foraminifer *Globigerinoides* spp. However, as shown in Figure 5a, an isotopic difference exists between these two groups.

[30] This offset could be explained by a difference in the season of calcification. Surface waters are subject to seasonal fluctuations associated with the development of seasonal thermocline and the vertical mixing. Consequently, these surface-dwelling plankton taxa can exhibit different chemical signals that reflect specific growth seasons. Because the calcification seasons of the modern analogs of these species fall between spring and late summer, this parameter might only display a slight influence on the registered isotopic shifts.

[31] Another candidate explanation for those isotopic differences is the uncertainties related to the vital-effect corrections applied. Serrano et al. [2007] established equivalences between the taxonomic categories of Pliocene assemblages and the recent ones. On this basis, they consider that *Globigerinoides ruber* (white form) and *Globigerinoides obliquus* are morphological variants of the same evolutionary species and as such, require the same ecologic preferences. For the quaternary planktic foraminifer *Globigerinoides ruber* in the Mediterranean, a vital effect of about  $-0.6\text{‰}$  have been estimated by Rohling et al. [2004]. Taking into account this hypothesis (Figure 5b), oxygen isotopic values of *G. obliquus* and *P. lacunosa* fall in the same range, supporting the idea that both taxa had the same habitat.

### 5.3. Reconstruction of Sea-Surface Temperature and Salinity Variations During Middle Pliocene Precession Cycles

[32] The oxygen isotopic composition of *Pseudoemiliana lacunosa* and *Orbulina universa* are higher in marly limestones than in sapropelic marls (Figure 5a). Similar results were obtained by Gudjonsson and Van der Zwaan [1985] on *Globigerinoides obliquus*. Since the pioneer work of Rossignol-Strick [1985], numerous studies have

considered that these negative  $\delta^{18}\text{O}$  excursions in sapropelic horizons reflect a freshening of surface water caused by enhanced river runoff and precipitation increase during the course of orbitally driven insolation changes.

[33] Because the  $\delta^{18}\text{O}$  of biogenic calcite is controlled both by seawater temperature and  $\delta^{18}\text{O}$  of seawater (i.e., salinity), we use the alkenone unsaturation ratios to determine the sea surface temperatures (SST) and evaluate the respective role of each parameter in the  $\Delta\delta^{18}\text{O}_{s-1}$  amplitude.

#### 5.3.1. Temperature Variations

[34] The use of the  $U_{37}^k$  index as a paleothermometer in ancient sediments is an open question because alkenone producers are unknown. Therefore the applicability of modern temperature equations for the reconstruction of past SST environments may be controversial. In order to find potential alkenone producers in the geological past, Marlowe et al. [1990] compared the simultaneous occurrence of alkenones and coccolithophorids in Cenozoic sediments from DSDP cores. Their results suggest that living species of the genus *Gephyrocapsa* are the main contributors of alkenones to contemporary marine sediments, and that the extinct genera of the family Noelaerhabdaceae were more likely sources of alkenones in the Tertiary and Pleistocene sediments. On this basis, *Pseudoemiliana lacunosa* and *Reticulofenestra* spp. represent possible sources of alkenones in our samples. In the present study, *Pseudoemiliana lacunosa* is the dominant coccolithophorid species belonging to the Noelaerhabdaceae family, so we will consider it as the major source of alkenones in our samples.

[35] The alkenone paleotemperature equation of Conte et al. [2006] ( $\text{SST}(\text{°C}) = -0.0957 + 54.293(U_{37}^k) - 52.894(U_{37}^k)^2 + 28.321(U_{37}^k)^3$ ) was used here to estimate the SSTs for our samples. The internal precision of the temperature estimate is  $0.5\text{°C}$ .

[36] The SST estimates indicate that the sapropelic layers formation coincided with a mean surface water warming compared to marly limestones deposit conditions (Figure 6). The temperatures range between  $26.4\text{°C}$  and  $27.6\text{°C}$  for the sapropelic marl layers and between  $23.8\text{°C}$  and  $26\text{°C}$  for the marly limestone beds (Figure 6). Paleoclimate modeling experiments show that the middle Pliocene represents a period significantly warmer than today. Midlatitude global sea-surface temperature estimations for this period are warmer by such as

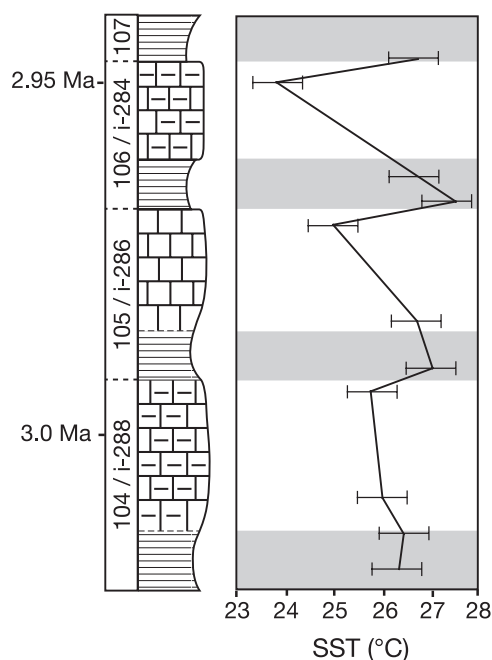


**Figure 6.** SST ( $^{\circ}\text{C}$ ) values determined by alkenone unsaturation ratio. SST values indicate that the sapropelic marls deposition occurred in warmer surface water conditions than the marly limestones.

3–4 $^{\circ}\text{C}$  [Cronin, 1991; Haywood et al., 2002]. In the modern Mediterranean, during the summer, the superficial waters in the Strait of Sicily can be strongly heated by insolation up to 26 $^{\circ}\text{C}$  [Levitus, 1982]. Thus the SSTs deduced from alkenone unsaturation index in the present study may reflect the mid-Pliocene summer SSTs according to the climatic models.

[37] Taking into account those temperature estimations recorded by *Pseudoemiliana lacunosa*, it appears that this species must have calcified very close to the sea-surface. If we consider the bathymetric distribution of the planktic species proposed in Figure 5a, this would imply that the planktic foraminifer *Globigerinoides obliquus* calcified in even warmer temperature conditions than coccoliths which is not consistent with the model predictions for Pliocene climate. The vital-effect proposed by Rohling et al. [2004] seems to be more appropriate for the species *G.obliquus*. Thus the depth habitat for the nannoplankters must be equivalent to that of surface-dwelling planktic foraminifer *Globigerinoides* spp.

[38] The amplitude of the temperature variations between the two lithologies varies for each cycle. It

is quite low for cycle 104 ( $\Delta T = 0.5^{\circ}\text{C}$ ), intermediate for cycle 105 ( $\Delta T = 2.3^{\circ}\text{C}$ ) and higher for cycle 106 ( $\Delta T = 3.8^{\circ}\text{C}$ ).

### 5.3.2. Estimates of the Sea-Surface $\delta^{18}\text{O}$ Variations During the Precession Cycles

[39] The coccolith  $\delta^{18}\text{O}$  records depend both on the SST and seawater  $\delta^{18}\text{O}$  ( $\delta w$ ) at the time of their growth. Using the alkenone-derived SST and *Pseudoemiliana lacunosa*  $\delta^{18}\text{O}$  records corrected from the vital effect following Ziveri et al. [2003], it is possible to estimate the  $\delta w$  variations by solving the Dudley and Nelson [1986] equation calibrated from laboratory cultures of *Emiliana huxleyi*:

$$T = 21.7 - 5(\delta c - \delta w), \quad (1)$$

where  $\delta c$  and  $\delta w$  are the  $\delta^{18}\text{O}$  values of coccolith calcite (V-PDB) and ambient seawater (V-SMOW), respectively.

[40] The calculated  $\delta w$  values (from  $-1.44\text{‰}$  to  $-0.5\text{‰}$  in the sapropelic marls and from  $-0.67\text{‰}$  to  $-0.16\text{‰}$  in the marly limestones), indicate cyclic lowerings in the sapropelic layers (Figure 7).

[41] These low  $\delta w$  values can be explained by a salinity decrease resulting from major changes in the freshwater budget in the Mediterranean Sea

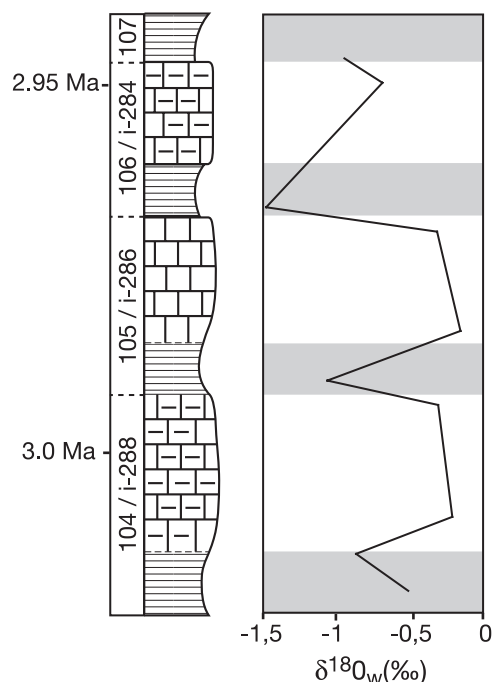


**Figure 7.** Evolution of seawater oxygen isotopic ratios ( $\text{‰}$  SMOW) throughout the studied section.

during the sapropel deposition. This assumption is in agreement with clay mineral analysis [Foucault and Mélières, 1995, 2000] and palynological data [Combourieu-Nebout et al., 2004].

### 5.3.3. Salinity Variations

[42] To estimate salinity variations from alkenone SSTs and  $\delta^{18}\text{O}$  values of *Pseudoemiliana lacunosa*, we used equation (2) [Rostek et al., 1993]. The specificity of our approach is the use of the same recorder for the temperature (alkenone) and  $\delta^{18}\text{O}_C$ : *Pseudoemiliana lacunosa* coccolith.

$$S = \Delta S_0 + S^* + (\Delta\delta^{18}\text{O}_C - a - b\Delta T)/c \quad (2)$$

S being past local salinity,  $S^*$  the present-day local salinity,  $\Delta\delta^{18}\text{O}_C$  corresponding to the difference in  $^{18}\text{O}/^{16}\text{O}$  composition of biogenic calcite between time  $t$  and present,  $\Delta S_0$  is the global change of ocean salinity due to ice shield growth. The correction parameter  $a$  represents time-dependant global variations of seawater  $\delta^{18}\text{O}$  related to ice volume changes [Volgelsang, 1990]. The constant  $b$  quantifies the temperature effect on  $\delta^{18}\text{O}_C$ . This coefficient links  $\delta^{18}\text{O}_C$  to  $\delta^{18}\text{O}_w$ . To estimate the isotopic change associated with temperature variations, we use the temperature independently estimated from the alkenone  $\text{U}_{37}^k$  values.  $\Delta T$  is the temperature difference between modern and past.

[43] The parameter  $b$  represents the slope of the linear relationship between alkenone SSTs and  $\delta^{18}\text{O}$  values of *Pseudoemiliana lacunosa*. According to our results, we use the value of  $-0.37$  for this parameter. The constant  $c$  is the slope of the linear relationship between  $\delta w$  and  $S$ . For the modern Mediterranean sea, the relationship between seawater  $\delta w$  and salinity was evaluated by Pierre [1999] as  $\delta w = (c * S) - 8.9$ , where  $S$  is salinity and  $-8.9$  represents the regional freshwater  $\delta w$ . For the modern Mediterranean sea, the slope  $c$  has a value of  $0.25$  [Pierre, 1999]. This parameter may have been different in the past, when different moisture sources provided freshwater to the Mediterranean [Rohling and Bigg, 1998]. To account for such possible changes during sapropel deposition, Emeis et al. [2000] used a steeper slope of  $0.45$ . This value, which is based on the assumption that the freshwater end-member during this period may have been much lighter in isotopic composition. An intermediate value of  $0.35$  is probably the best value to be used in equation (2) to quantify the salinity variations [Emeis et al., 2000].

[44] Uncertainties still exist for Pliocene climates. On the one hand, Hilgen et al. [1993] consider that the northern ice sheets were reduced and stable over the studied period, implying no significant “glacial” effects during the short timescale considered for this study. On the other hand, Loutre and Berger [2005] indicate the occurrence of three glaciations between 3 and 2 Ma, and Caruso [2004] showed that the period between 2.57 and 2.4 Ma coincides with the expansion of the northern hemisphere ice sheet. As an analogy to Pleistocene climate, our study time interval could then correspond to interglacial conditions. Below, we discuss two possible scenarios:

[45] 1. Following the hypothesis of Hilgen et al. [1993], that neglects glacial effects, both parameters  $\Delta S_0$  and  $a$  are constant throughout our time interval. For the sapropelic marls (s), equation (2) would give

$$S_s = \Delta S_0 + S^* + ((\delta^{18}\text{O}_{Cs}(t) - \delta^{18}\text{O}_{Cs}(0)) - a - b(T_s - T_0))/c \quad (3)$$

and for the marly limestones (l)

$$S_l = \Delta S_0 + S^* + ((\delta^{18}\text{O}_{Cl}(t) - \delta^{18}\text{O}_{Cl}(0)) - a - b(T_l - T_0))/c \quad (4)$$

From equations (3) and (4), it is possible to calculate the salinity variation between the sapropelic marls and marly limestones using the following equation:

$$S_s - S_l = ((\delta^{18}\text{O}_{Cs}(t) - \delta^{18}\text{O}_{Cl}(t)) - b(T_s - T_l))/c \quad (5)$$

Consequently, the salinity shifts between the sapropelic marls and marly limestones recorded by *P. lacunosa* in the three cycles studied, vary between  $-1$  for cycle 104 to  $-0.37$  for cycle 106.

[46] 2. Taking into account “glacial” effects,  $\Delta S_0$  and  $a$  ought not to be constant throughout these Pliocene cycles, equation (5) becomes

$$S_s - S_l = ((\delta^{18}\text{O}_{Cs}(t) - \delta^{18}\text{O}_{Cl}(t)) - b(T_s - T_l))/c - \Delta a/c + (\Delta(\Delta S_0)) \quad (6)$$

where  $\Delta a$  represents the global variations of seawater  $\delta^{18}\text{O}$  and  $\Delta(\Delta S_0)$  represents the global change of ocean salinity related to ice volume changes during a precession cycle. The salinity change due to ice volume variations was estimated assuming that salinity increased

**Table 3.** Temperature and Salinity Variations Between Sapropelic Marls and Marly Limestones for the Three Cycles Studied<sup>a</sup>

Cycles	Temperature Variations (s – l)	Salinity Variations (s – l)	
		Equation (5)	Equation (6)
104	0.7°C	–1	–1.2
105	2.4°C	–0.6	–0.6
106	4.1°C	–0.3	–0.2

<sup>a</sup>Notes: s, sapropelic marls; l, marly limestones. Temperature variations are expressed in °C and deduced from alkenone unsaturation ratios. Salinity variations (equation (5) and equation (6)) are the results obtained assuming no glacial effects throughout the cycles and taking into account glacial effects, respectively.

by 1 when the seawater  $\delta^{18}\text{O}$  increased by 1.2‰ [Labeyrie et al., 1987; Shackleton, 1987; Fairbanks, 1989]. As we have previously determined the  $\delta w$  fluctuations throughout the section studied (Figure 6), it is then possible to calculate the  $\Delta$  ( $\Delta S_0$ ) parameter for each cycle. We use the mean value of  $\Delta a = 0.2$  from Pleistocene precession cycles [Labeyrie et al., 1987]. Consequently, the amplitude of salinity change (Table 3) estimated from equation (6), between the sapropelic marls and the marly limestones varies then between –1.2 for cycle 104 to –0.2 for cycle 106, which is close to the estimations obtained considering no glacial effects.

[47] Regardless of the “glacial effects”, our results show that the salinity effect is more important during cycle 104 in comparison with cycles 105 and 106. During cycle 106, the salinity variations are very weak.

## 6. Summary and Conclusions

[48] This study, focused on three mid-Pliocene precession cycles from the Punta Piccola section, clearly shows the potential of coccolith isotopic ratios in paleoceanography. We present here, for the first time, paleoenvironmental reconstructions based on the use of monospecific coccolith  $\delta^{18}\text{O}$  (*P.lacunosa*) and  $\text{U}_{37}^{\text{K}}$ -derived temperatures.

[49] The results show a difference in magnitude of the temperature and salinity shifts estimated in each of the three cycles studied here and suggest that these deposits may have formed under a variety of paleoceanographic conditions. For cycle 104 (i-288), the influence of freshwater and, consequently, of reduced salinity may have significantly influenced the uppermost part of the water column. For cycle 105 (i-286), both temperature and salinity variations have affected the sea-surface

and, as shown for the cycle 106 (i-284), only a minor salinity variation is detected, whereas temperature variations are strong. Our results show that salinity variations do not appear to be the dominant environmental parameter associated with the formation of these deposits. However, the environmental reconstructions published by Foucault and Mélières [1995, 2000] based on clay minerals assemblages and by Combourieu-Nebout et al. [2004] on palynological data indicate that the sedimentary cycles of Punta Piccola are closely linked to the African monsoonal climate system.

[50] According to deMenocal [2004], the African climate changed after the closure of the Isthmus of Panama (4.4–4.6 Ma [Haug et al., 2001]) which is associated with the gradual onset of high-latitude glacial cycles at 3.2–2.6 Ma.

[51] Prior to 2.8 Ma, the subtropical African climate varied following the 23–19 kyr cyclicity which has been interpreted to reflect African monsoonal variability resulting from low-latitude, precessional insolation forcing. At 2.8 ( $\pm 0.2$ ) Ma, the African climate started to vary primarily following the longer 41 kyr period [Shackleton et al., 1990; Raymo, 1994; Ruddiman et al., 1989] with the onset of glacial ice rafting.

[52] The Punta Piccola sedimentary cycles investigated in this study are dated between 3.01 and 2.9 Ma and were deposited during the onset of the obliquity cycles. According to these observations, precession might have been the fundamental driver of African monsoonal climate throughout the deposition of Punta Piccola sedimentary cycles. Nevertheless, high-latitude glacial cooling and drying effects of the African climate could have been superimposed on this signal and recorded in the oxygen isotopic data of coccoliths from the cycle 106. The interference between obliquity and precession have previously been notified in the western Mediterranean orbitally controlled deposits from the Sorbas basin (Southeast Spain). Sierra et al. [2003] show that the variability of foraminifera assemblages in this section is closely linked to the interaction of these astronomical forcings and the sensitivity of the system due to the semi-isolation of the Mediterranean basin.

[53] We are aware that the low resolution of the sampling does not allow a detailed full reconstruction of the short-scale changes occurring within the sapropelic and marly limestones layers. To reach such a temporal resolution, the next challenge will be the reduction of sample quantities needed to

obtain pure fractions using the separation technique. Nevertheless, this study provides a new step-forward in the use of isotopic composition of monospecific coccolith fractions in paleoceanographic studies.

## Acknowledgments

[54] We would like to thank Nathalie Labourdette (Laboratoire Biominéralisations et Paléoenvironnements, UPMC) for her efficient technical assistance. We are grateful to A. Foucault (MNHN, Département de Géologie, Paris) for the discovery of the Pliocene outcrops in South Sicily. This manuscript benefited greatly from the critical reviews made by the anonymous reviewers. A special thanks to P. Dedecker (Department of Geology, University of Canberra, Australia) for his helpful comments on the manuscript and for his suggestions concerning the English form. This study was financially supported by UPMC research grants (BQR 2004/2006). This is LCSE contribution 2299.

## References

- Bemis, B. E., H. J. Spero, D. W. Lea, and J. Bijma (2000), Temperature influence on the carbon isotopic composition of *Globigerina bulloides* and *Orbulina universa* (planktonic foraminifera), *Mar. Micropaleontol.*, **38**, 213–228.
- Bernasconi, S. M., and M. Pika-Biolzi (2000), A stable isotope study of multiple species of planktonic foraminifera across sapropels of the Tyrrhenian Sea, ODP Site 974, *Palaeogeogr. Palaeoclimatol. Palaeoecol.*, **158**, 281–292.
- Bown, P. R., (Ed.) (1998), *Calcareous Nannofossil Biostratigraphy*, CRC Press, Boca Raton, Fla.
- Brassell, S. C., G. Eglinton, I. Marlowe, U. Pflaumann, and M. Sarnthein (1986), Molecular stratigraphy: A new tool for climatic assessment, *Nature*, **320**, 129–133.
- Broerse, A. T. C., P. Ziveri, J. E. Van Hinte, and S. Honjo (2000), Coccolithophore export production, species composition, and coccolith- $\text{CaCO}_3$  fluxes in the NE Atlantic ( $34^\circ\text{N}$   $21^\circ\text{W}$  and  $48^\circ\text{N}$   $21^\circ\text{W}$ ), *Deep Sea Res., Part II*, **47**, 1877–1905.
- Brolsma, M. J. (1978), Quantitative foraminiferal analysis and environmental interpretation of the Pliocene and topmost Miocene on the South coast of Sicily, *Utrecht Micropaleontol. Bull.*, **18**, 159 pp.
- Caruso, A. (2004), Climatic changes during Late Pliocene and Early Pleistocene at Capo Rossello (Sicily, Italy): response from planktonic foraminifera, in *Proceedings of the First Italian Meeting on Environmental Micropaleontology*, Grzybowski Foundation Spec. Publ., vol. 9, edited by R. Coccioni, S. Galeotti, and F. Lirer, pp. 17–36, Grzybowski Found., London.
- Cita, M. B., and S. Gartner (1973), Studi sul Pliocene e sugli strati del passaggio dal Miocene al Pliocene, IV. The stratotype Zanlean. Foraminiferal and nannofossil biostratigraphy, *Riv. Ital. Paleontol. Stratigr.*, **79**, 503–558.
- Combourieu-Nebout, N., A. Foucault, and F. Mélières (2004), Vegetation markers of palaeoclimate cyclical changes in the Pliocene of Punta Piccola (Sicily, Italy), *Palaeogeogr. Palaeoclimatol. Palaeoecol.*, **214**, 55–66.
- Conte, M. H., M.-A. Sicre, C. Rühlemann, J. C. Weber, S. Schulte, D. Schulz-Bull, and T. Blanz (2006), Global temperature calibration of the alkenone unsaturation index ( $U_{37}^K$ ) in surface waters and comparison with surface sediments, *Geochem. Geophys. Geosyst.*, **7**, Q02005, doi:10.1029/2005GC001054.
- Cronin, T. M. (1991), Pliocene shallow water paleoceanography of the North Atlantic Ocean based on marine ostracodes, *Quat. Sci. Rev.*, **10**, 175–188.
- deMenocal, P. B. (2004), Frontiers African climate change and faunal evolution during the Pliocene-Pleistocene, *Earth Planet. Sci. Lett.*, **220**, 3–24.
- Dudley, W. C., and C. S. Nelson (1989), Quaternary surface-water stable isotope signal from calcareous nannofossils at DSDP Site 593, southern Tasman Sea, *Mar. Micropaleontol.*, **13**, 353–373.
- Dudley, W. C., J. C. Duplessy, P. L. Blackwelder, L. E. Brand, and R. R. L. Guillard (1980), Coccoliths in Pleistocene-Holocene nannofossil assemblages, *Nature*, **285**, 222–223.
- Dudley, W. C., P. L. Blackwelder, L. E. Brand, and J. C. Duplessy (1986), Stable isotopic composition of coccoliths, *Mar. Micropaleontol.*, **10**, 1–8.
- Emeis, K. C., U. Struck, H. M. Schulz, R. Rosenberg, S. Bernasconi, H. Erlenkeuser, T. Sakamoto, and F. Martinez-Ruiz (2000), Temperature and salinity variations of Mediterranean Sea surface waters over the last 16 000 years from records of planktonic stable isotopes and alkenone unsaturation ratios, *Palaeogeogr. Palaeoclimatol. Palaeoecol.*, **158**, 259–280.
- Erez, J., and S. Honjo (1981), Comparison of isotopic composition of planktonic foraminifera in plankton tows, sediment traps and sediments, *Palaeogeogr. Palaeoclimatol. Palaeoecol.*, **33**, 129–156.
- Erez, J., and B. Luz (1983), Experimental paleotemperature equation for planktonic foraminifera, *Geochim. Cosmochim. Acta*, **47**, 1025–1031.
- Fairbanks, R. G. (1989), A 17000 year glacio-eustatic sea level record: influence of glacial melting rates on the Younger Dryas event and deep ocean circulation, *Nature*, **342**, 637–642.
- Fairbanks, R. G., and P. H. Wiebe (1980), Foraminifera and chlorophyll maximum: vertical distribution, seasonal succession, and paleoceanographic significance, *Science*, **209**, 1524–1526.
- Foucault, A., and F. Mélières (1995), Nature et origine des cycles sédimentaires métriques du Pliocène de l'ouest méditerranéen d'après l'étude du contenu terrigène de la Formation Narbone (Punta Piccola, Sicile, Italie), *C. R. Acad. Sci. Paris*, **321**, 869–876.
- Foucault, A., and F. Mélières (2000), Palaeoclimatic cyclicity in central Mediterranean Pliocene sediments: the mineralogical signal, *Palaeogeogr. Palaeoclimatol. Palaeoecol.*, **158**, 311–323.
- Goodney, D. E., S. V. Margolis, W. C. Dudley, P. Kroopnick, and D. F. Williams (1980), Oxygen and carbon isotopes of recent calcareous nannofossils as paleoceanographic indicators, *Mar. Micropaleontol.*, **5**, 31–42.
- Gudjonsson, L., and G. J. Van der Zwaan (1985), Anoxic events in the Pliocene Mediterranean, *Proc. K. Ned. Akad. Wet., Ser. B*, **88**, 69–82.
- Haidar, T. T., and H. R. Thierstein (2001), Coccolithophore dynamics off Bermuda (N. Atlantic), *Deep Sea Res., Part II*, **48**, 1925–1956.
- Haug, G. H., R. Tiedemann, R. Zahn, and A. C. Ravelo (2001), Pole of Panama uplift on oceanic freshwater balance, *Geology*, **29**, 207–210.

- Haywood, A. M., P. J. Valdes, and B. W. Sellwood (2002), Magnitude of middle Pliocene climate variability: A palaeoclimate modelling study, *Palaeogeogr. Palaeoclimatol. Palaeoecol.*, *188*, 1–24.
- Hilgen, F. J. (1987), Sedimentary rhythms and high resolution chronostratigraphic correlations in the Mediterranean Pliocene, *Newsl. Stratigr.*, *17*, 109–127.
- Hilgen, F. J. (1991), Astronomical calibration of Gauss to Matuyama sapropels in the Mediterranean and implication for the Geomagnetic Polarity Time Scale, *Earth Planet. Sci. Lett.*, *104*, 226–244.
- Hilgen, H. J., L. J. Lourens, A. Berger, and M. F. Loutre (1993), Evaluation of the astronomically calibrated time scale for the late Pliocene and the earliest Pleistocene, *Paleoceanography*, *8*, 543–565.
- Howell, M. W., R. C. Thunell, E. Di Stefano, R. Sprovieri, E. J. Tappa, and T. Sakamoto (1998), Stable isotope chronology and paleoceanographic history of sites 963 and 964, Eastern Mediterranean Sea, *Proc Ocean Drill. Program Sci. Results*, *160*, 167–180.
- Kidd, R. B., M. B. Cita, and W. B. F. Ryan (1978), The stratigraphy of eastern Mediterranean sapropel sequences recovered by DSDP Leg 42A and their paleoenvironmental significance, *Initial Rep. Deep Sea Drill. Proj.*, *42A*, 421–443.
- Kullenberg, B. (1952), On the salinity of water contained in marine sediments, *Göteborgs Kungl. Vitter. Handl., Ser. B*, *6*, 3–37.
- Labeyrie, L. D., J. C. Duplessy, and P. L. Blanc (1987), Variations in mode of formation and temperature of oceanic deep waters over the past 125,000 years, *Nature*, *327*, 477–482.
- Langereis, C. G., and F. J. Hilgen (1991), The Rosello composite: A Mediterranean and global reference section for the early to early late Pliocene, *Earth Planet. Sci. Lett.*, *104*, 211–225.
- Levitus, S. (1982), *Climatological Atlas of the World Ocean*, NOAA Prof. Pap. 13, 173 pp., U. S. Govt. Print. Off., Washington, D. C.
- Lourens, L. J., A. Antonarakou, F. J. Hilgen, A. A. M. Van Hoof, C. Vergnaud-Grazzini, and W. J. Zachariasse (1996), Evaluation of the Plio-Pleistocene astronomical timescale, *Paleoceanography*, *11*, 391–413.
- Loutre, M. F., and A. Berger (2005), Insolation, CO<sub>2</sub> et précipitations en période interglaciaire, *C. R. Geosci.*, *337*, 69–78.
- Marlowe, I. T., S. C. Brassell, G. Eglinton, and J. C. Green (1990), Long-chain alkenones and alkyl alkenoates and the fossil coccolith record of marine sediments, *Chem. Geol.*, *88*, 349–375.
- Mattioli, E., and B. Pittet (2002), Contribution of calcareous nannoplankton to carbonate deposition: A new approach applied to the Lower Jurassic of central Italy, *Mar. Micropaleontol.*, *45*, 175–190.
- Minoletti, F. (2002), Mise au point d'un protocole de séparation des assemblages de nannofossiles calcaires. Apports à la micropaléontologie et à la géochimie des producteurs carbonatés pélagiques. Application à la crise Crétacé-Tertiaire, Ph.D., Univ. Pierre et Marie Curie, Paris.
- Minoletti, F., S. Gardin, E. Nicot, M. Renard, and S. Spezzaferri (2001), Mise au point d'un protocole expérimental de séparation granulométrique d'assemblages de nannofossiles calcaires: Application paléocéologique et géochimique, *Bull. Soc. Géol. Fr.*, *172*, 437–446.
- Minoletti, F., M. de Rafelis, M. Renard, S. Gardin, and J. Young (2005), Changes in the pelagic fine fraction carbonate sedimentation during the Cretaceous–Paleocene transition: Contribution of the separation technique to the study of Bidart section, *Palaeogeogr. Palaeoclimatol. Palaeoecol.*, *216*, 119–137.
- Noël, D., G. Busson, A. Cornée, Y. Bodeur, and A. M. Mangin (1994), Contribution fondamentale des coccolithophoridés à la constitution des calcaires fins pélagiques du Jurassique moyen et supérieur, *Geobios*, *17*, 701–721.
- Okada, H., and S. Honjo (1973), The distribution of oceanic coccolithophorids in the Pacific, *Deep Sea Res. Oceanogr. Abstr.*, *20*, 355–374.
- Ortiz, J. D., A. C. Mix, W. Rugh, J. M. Watkins, and R. W. Collier (1996), Deep-dwelling planktonic foraminifera of the northeastern Pacific Ocean reveal environmental control of oxygen and carbon isotopic disequilibria, *Geochim. Cosmochim. Acta*, *60*, 4509–4523.
- Pearson, P. N., and N. J. Shackleton (1995), Neogene multi-species planktonic foraminifer stable isotope record, Site 871, Limalok Guyot, *Proc. Ocean Drill. Program Sci. Results*, *144*, 401–410.
- Pierre, C. (1999), The oxygen and carbon isotope distribution in the Mediterranean water masses, *Mar. Geol.*, *153*, 41–55.
- Ravelo, A. C., and R. G. Fairbanks (1992), Oxygen isotopic composition of multiple species of planktonic foraminifera: Records of the modern photic zone temperature gradient, *Paleoceanography*, *7*, 815–831.
- Raymo, M. E. (1994), The initiation of Northern Hemisphere glaciation, *Annu. Rev. Earth Planet. Sci.*, *22*, 353–383.
- Reid, F. M. H. (1980), Coccolithophorids of the North Pacific Central Gyre with notes on their vertical and seasonal distribution, *Micropaleontology*, *26*, 151–176.
- Rohling, E. J. (1994), Review and new aspects concerning the formation of eastern Mediterranean sapropels, *Mar. Geol.*, *122*, 1–28.
- Rohling, E. J., and G. R. Bigg (1998), Paleosalinity and  $\delta^{18}O$ : A critical assessment, *J. Geophys. Res.*, *103*, 1307–1318.
- Rohling, E. J., and W. W. C. Gieskes (1989), Late Quaternary changes in Mediterranean intermediate water density and formation rate, *Paleoceanography*, *4*, 531–545.
- Rohling, E. J., and F. J. Hilgen (1991), The eastern Mediterranean climate at times of sapropel formation: A review, *Geol. Mijnbouw*, *70*, 253–264.
- Rohling, E. J., et al. (2004), Reconstructing past planktic foraminiferal habitats using stable isotope data: a case history for Mediterranean sapropel S5, *Mar. Micropaleontol.*, *50*, 89–123.
- Rossignol-Strick, M. (1983), African monsoons, an immediate climate response to orbital insolation, *Nature*, *304*, 46–49.
- Rossignol-Strick, M. (1985), Mediterranean Quaternary sapropels, an immediate response of the African monsoon to variations of insolation, *Palaeogeogr. Palaeoclimatol. Palaeoecol.*, *49*, 237–263.
- Rostek, F., G. Ruhland, F. Bassinot, P. J. Müller, L. D. Labeyrie, Y. Lancelot, and E. Bard (1993), Reconstructing sea surface temperature and salinity using  $\delta^{18}O$  and alkenone records, *Nature*, *364*, 319–321.
- Ruddiman, W. F., M. E. Raymo, D. G. Martinson, B. M. Clement, and J. Backman (1989), Pleistocene evolution: Northern Hemisphere ice sheets and North Atlantic Ocean, *Paleoceanography*, *4*, 353–412.
- Serrano, F., J. M. Gonzalez-Donoso, P. Palmqvist, A. Guerra-Merchan, D. Linares, and J. A. Perez-Claros (2007), Estimating Pliocene sea-surface temperatures in the Mediterranean: An approach based on the modern analogs technique, *Palaeogeogr. Palaeoclimatol. Palaeoecol.*, *243*(1–2), 174–188.
- Shackleton, N. J. (1987), Oxygen isotopes, ice volume and sea-level, *Quat. Sci. Rev.*, *6*, 183–190.

- Shackleton, N. J., A. Berger, and W. R. Peltier (1990), An alternative astronomical calibration of the lower Pleistocene time-scale based on ODP Site 677, *Trans. R. Soc. Edinburgh Earth Sci.*, *81*, 251–261.
- Sierro, F. J., J. A. Flores, G. Francés, A. Vazquez, R. Utrilla, I. Zamarreño, H. Erlenkeuser, and M. A. Barcena (2003), Orbitally-controlled oscillations in planktic communities and cyclic changes in western Mediterranean hydrography during the Messinian, *Palaeogeogr. Palaeoclimatol. Palaeoecol.*, *190*, 289–316.
- Spaak, P. (1983), Accuracy in correlation and ecological aspects of the planktonic foraminiferal zonation of the Mediterranean Pliocene, *Utrecht Micropaleontol. Bull.*, *28*, 159 pp..
- Spero, H. J., and D. W. Lea (1996), Experimental determination of stable isotope variability in *Globigerina bulloides*: Implications for paleoceanographic reconstructions, *Mar. Micropaleontol.*, *28*, 231–246.
- Sprovieri, R., M. Sprovieri, A. Caruso, N. Pelosi, S. Bonomo, and L. Ferraro (2006), Astronomic forcing on the planktonic foraminifera assemblage in the Piacenzian Punta Piccola section (southern Italy), *Paleoceanography*, *21*, PA4204, doi:10.1029/2006PA001268.
- Stoll, H. M., and S. Bains (2003), Coccolith Sr/Ca records of productivity during the Paleocene-Eocene thermal maximum from the Weddell Sea, *Paleoceanography*, *18*(2), 1049, doi:10.1029/2002PA000875.
- Ternois, Y., M.-A. Sicre, A. Boireau, M. H. Conte, and G. Eglinton (1997), Evaluation of long-chain alkenones as paleo-temperature indicators in the Mediterranean sea, *Deep Sea Res., Part I*, *44*, 271–286.
- Thierstein, H. R., and P. H. Roth (1991), Stable isotopic and carbonate cyclicity in Lower Cretaceous deep-sea sediments: dominance of diagenetic effects, *Mar. Geol.*, *97*, 1–34.
- Van der Zwaan, G. J., and L. Gudjonsson (1986), Middle Miocene-Pliocene stable isotope stratigraphy and paleoceanography of the Mediterranean, *Mar. Micropaleontol.*, *10*, 71–90.
- Volgelsang, E. (1990), Paläo-Ozeanographie des Europäischen Nordmeeres an Hand stabiler Kohlenstoff- und Sauerstoffisotope, Ph.D., Univ. Kiel, Kiel, Germany.
- Ziveri, P., H. Stoll, I. Probert, C. Klaas, M. Geisen, G. Ganssen, and J. Young (2003), Stable isotope 'vital effects' in coccolith calcite, *Earth Planet. Sci. Lett.*, *210*, 137–149.